RSC Advances

PAPER

View Article Online
View Journal | View Issue

Cite this: *RSC Adv.*, 2024, **14**, 3202

Influence of oxygen content on selective laser melting leading to the formation of spheroidization in additive manufacturing technology

Jibing Chen, * Yong She, Xinyu Du, Yanfeng Liu, Yang Yang and Junsheng Yang

Selective laser melting (SLM) additive manufacturing technology with different oxygen contents leads to the appearance of spherical solids of different sizes on the surface of the part, which affects the mechanical properties of the part, surface roughness, *etc.* In this study, the SLM molding technique was applied using three different 316L metal powders with different oxygen contents. The spheroidization properties and morphology of the samples were observed using a Quanta 200 environmental scanning electron microscope (ESEM), and the samples were observed microscopically and subjected to EDX spectroscopy using metallographic microscopy, and the mechanical properties were investigated. The results of the study showed that when using gas atomized powders, no spheroidization occurred when the oxygen content of the powders was 5.44 ± 0.01% in all cases, whereas using water atomized powders produced spherical structures with larger dimensions. This observation was closely related to the shape and particle size of the powder. When 316L metal powder with an oxygen content of 4.52 ± 0.01% was used for molding, small spherical structures appeared on the surface of the samples. When metal powder with an oxygen content of 5.44 ± 0.01% was used for the molding, larger spherical structures appeared on the surface of the samples. When the powder with an oxygen content of 5.90 ± 0.01% was used for the molding, more small spherical structures and some large spherical structures appeared on the surface of the samples. This suggests that higher oxygen levels may inhibit the occurrence of spheroidization. EDX spectroscopic analysis revealed that the white matter on the surface of the samples without spheroidization was mainly composed of Fe and Cr, whereas the white matter on the surface of the large-sized spherical structures was mainly composed of Si and Mn, which may be related to the oxygenophilicity of the various substances.

Received 18th December 2023
Accepted 20th December 2023

DOI: 10.1039/d3ra08627e

rsc.li/rsc-advances

1 Introduction

Based on the demand for the rapid manufacturing of complex high-performance metal parts, the rapid prototyping technology selective laser melting (SLM), one of the newest forms of rapid prototyping and manufacturing (RP&M), was born. The basic idea of SLM forming technology is the same as that of other rapid forming technologies and is based on the idea of stacked manufacturing, in which a CAD model is first created and the prototype of the part is then sliced layer by layer, where each layer contains a cross-section.[1–3] Each layer of the part includes geometric information of the cross-section that is used to generate a file in STL format. Then, the metal powder in the cut area is melted using a high-energy laser beam under computer control, and the growth manufacturing principle is used to form the metal parts, which has the advantages of producing complex shapes, high relative density and saving materials.[4]

At present, SLM technology is used at home and abroad in the production of key components in aerospace, biomedicine, military equipment, and other fields and has achieved some results and has become an important development direction for RP&M technology. However, because SLM involves complex physicochemical metallurgical and other processes, the forming process is prone to defects, such as spheroidization, porosity, and cracks.[5] At the same time, the variety of molding materials is also limited. These factors significantly affect the promotion and application of SLM technology. In fact, the above-mentioned forming errors of SLM involve several important theoretical problems.[6] Therefore, an in-depth study of the key theoretical issues of the SLM forming process is of great theoretical value and practical significance for the development of SLM technology and for improving its practicality.

Spheroidization in selective laser melting is the formation of spherical molten droplets that atomize on the surface of the material during the laser melting process. This phenomenon often occurs during the laser melting of metals, ceramics, and other materials. The mechanism of the spheroidization phenomenon is that when the liquid metal is irradiated by the laser, the metal powder is melted due to the laser energy, and the

School of Mechanical Engineering, Wuhan Polytechnic University, Wuhan 430023, China. E-mail: jbchen@whpu.edu.cn

molten liquid metal splashes due to the impact of the laser and the pressure difference in the melt pool, thereby producing small droplets,[7,8] which can form spherical solids that adhere to the surface of the parts after cooling. Due to the difference in oxygen content, a high oxygen content produces large solid spheres, whereas a lower oxygen content produces small solid spheres, the diameter of which ranges from tens of micrometers to hundreds of micrometers, which seriously affects the quality, mechanical properties, smoothness, and uniformity of the parts.[9,10] Therefore, reducing the spheroidization phenomenon is of great importance for optimizing the selective laser melting process. Therefore, it is particularly important to investigate and solve the phenomenon of spheroidization. In recent years, the problem of spheroidization in selective laser melting rapid prototyping technology has attracted the attention of many scientists and has become a hot spot in the field of SLM research.[11–14]

Currently, there are few studies on the influence of the oxygen content on the spheroidization phenomenon in SLM rapid prototyping technology.[15–18] Among the few studies, Li *et al.*[19] suggested that the reason for the spheroidization problem is a wetting problem between the liquid metal and the solid surface but did not indicate whether this was related to the oxygen content. Zhang *et al.*,[20] when studying the SLM spheroidization problem, found that the size of the metal balls in the melt pool was related to the oxygen content and that the size of the metal balls in the melt pool increased with increasing the oxygen content. Kruth *et al.*[21,22] found that the spheroidization phenomenon was inextricably linked to surface oxidation and that the formation of spheroidization was inseparable from surface oxidation, and also that the generated oxide film could be broken with a higher energy laser or by adding a deoxidizer to the liquid metal to stop the occurrence of spheroidization. In summary, the problem of spheroidization in SLM has been a research hotspot for scientists, but its relation to the oxygen content has rarely been mentioned. Therefore, three different preparations of 316L metal powders are presented in this study. Different forms of powder have been used for SLM forming.[23–25] Using the 316L metal powder with an oxygen content of 4.52 ± 0.01% produced large spherical solids during the forming process, while using 316L metal powder with an oxygen content of 5.44 ± 0.01% did not produce large spherical solids during the forming process. Also, the use of 316L metal powder with an oxygen content of 5.90 ± 0.01% did not produce large spherical solids during the forming process. It can be seen that the spherical solids produced during SLM molding increased with increasing the oxygen content; however a high oxygen content inhibited the formation of spheroidization and the small spheres produced were independent of the oxygen content.

2 Experimental

2.1 Materials and preparation

316L stainless steel has good mechanical properties, strong oxidation resistance, and a wide range of sources. Many powder manufacturers provide a spot supply, so the price is also very low. In addition, there are many studies on its sintering at home and abroad, as the sintering process is relatively mature, and it is an ideal metal material. The chemical composition is shown in Table 1. Fig. 1 shows a SEM image of 316L stainless steel powder. It can be seen from the figure that the spherical particles of 316L stainless steel powder were fewer, and that most of the particles were irregular in shape, the surface was angular, the particle size was uneven, whereby a few of the particles were relatively large while the fine particles agglomerated, which was a result of the particle surface energy.[26–28] In this experiment, three types of 316L stainless steel powders (AISI316L) were selected for SLM forming and were mainly investigated based on the following two points: (1) the influence of different powder properties on the spheroidization of SLM forming; (2) for the same type of powder, the influence of different forming processes on the spheroidization of the powder forms. The properties of the three powders selected for this experiment are shown in Table 2.

2.2 Water atomized powder

Water atomization, *i.e.*, the use of high pressure water to atomize liquid metal into a large number of small droplets, causes solidification and forms a metal powder.[29] The powders tested here were two kinds of commercial 316L stainless steel powder provided by Beijing Wardley Company. The microscopic morphology of the first powder is shown in Fig. 2a and b. It can be seen that the particle shape of the powder was mostly irregular, and only a small amount of powder has a nearly spherical shape. Fig. 2c shows the particle size distribution of the powder, and it can be seen that the particle size of the powder was mainly distributed between 5 and 75 μm.[30]

Fig. 3 shows the microscopic morphology and particle-size distribution of the second water-atomized 316L stainless steel powder. It can be seen that the powder was completely irregular in shape and there were nearly no spherical powder particles (Fig. 3a and b). The particle size of the powder was predominantly between 5 and 90 μm (Fig. 3c).

Table 1 Chemical composition of the 316L stainless steel

Elements	Fe	Cr	Ni	C	Mn	Si	P	S	Mo
Content (%)	Bal.	17	17	0.08	2.0	1.0	0.045	0.03	2.5

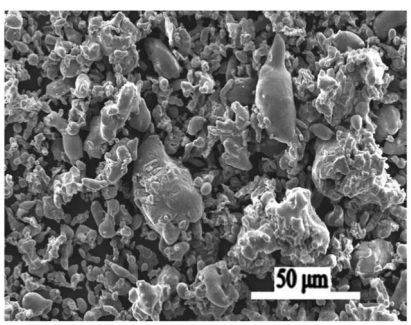

Fig. 1 SEM image of 316L stainless steel particles.

Table 2 Three 316L stainless steel powders studied with different properties

Powder number	Preparation method	Preparation site	Powder shape	Average particle size	Oxygen content (at%)
1#	Water atomization method	Beijing Wardrobe Company	Irregular	27 μm	5.44
2#	Water atomization method	Beijing Wardrobe Company	Irregular	34 μm	5.90
3#	Aerosolization method	CSU	Ball-shaped	20 μm	4.52

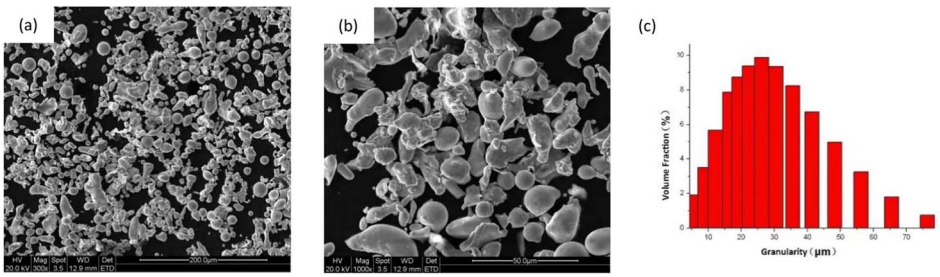

Fig. 2 Water atomized 316L stainless steel powder. (1#) Morphology and particle-size distribution: (a) and (b) powder micro-morphology; (c) powder particle-size distribution.

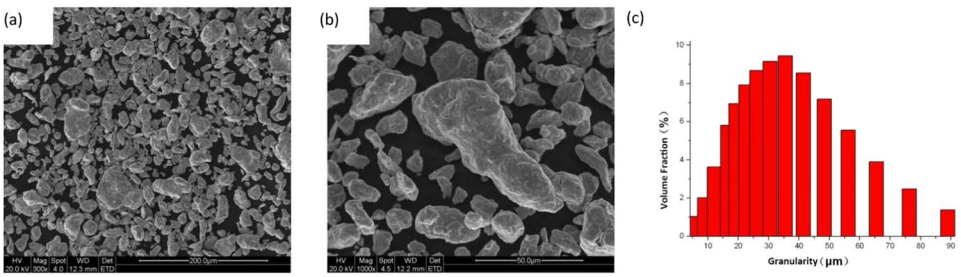

Fig. 3 Morphology and particle-size distribution of water atomized 316L stainless steel powder (2#): (a) and (b) powder micro-morphology; (c) powder particle-size distribution.

2.3 Aerosolized powder

The basic principle of producing aerosolized powder is to use a high-speed gas stream to impinge on the flowing liquid metal so that the kinetic energy of the gas converts the material into a large number of tiny melt particles with high surface energy, and the melt particles then solidify to form metal powder particles.[31] Aerosolized powders have the advantages of a low oxygen content and high sphericity. The aerosolized 316L stainless steel powder used in this experiment was produced in the State Key Laboratory of Powder Metallurgy, Central South University (CSU), and its micromorphology is shown in Fig. 4. It can be seen that the powder particles were spherical with a wide particle-size distribution (about 3–40 m). The energy spectrum test showed that the molar oxygen content in the powder was 4.52%.

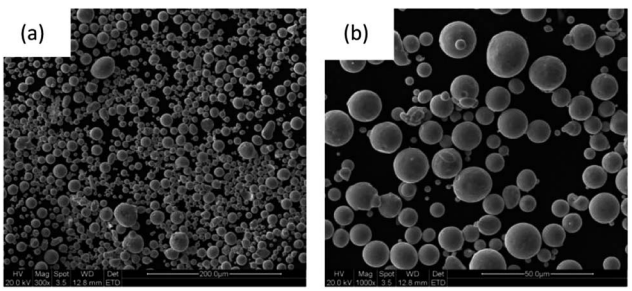

Fig. 4 Microscopic morphology of 316L stainless steel powder prepared by aerosolization: (a) ×300, (b) ×1000.

2.4 Experimental equipment

The test equipment involved a BLT-A160 metal powder selective laser forming machine developed by our Platinum Lite group, as shown in Fig. 5. Table 3 shows the parameters of the device.

2.5 Characterization methods

The spheroidization properties and morphology of the samples (both line and area spheroidization) were observed using a Quanta 200 environmental scanning electron microscope (ESEM) (FEI). The conventional procedure was followed to prepare metallographic samples to study the properties of the longitudinal section of the individual melt channel. Aqua regia was chosen as the metallographic etchant, and the etching time was approximately 30 s. The microstructure was observed using an Axiovert 200 MAT metallographic microscope.

Fig. 5 Experimental equipment of SLM.

Table 3 Parameters of BLT-A160

Model	BLT-A160
Forming space ($L \times W \times H$)	160 mm × 160 mm × 100 mm
Laser power	500 W
Laser wavelength	1060–1080 nm
Layering thickness	10–40 μm
Maximum scanning speed	7 m s^{-1}
Forming efficiency	15 cm^3 h^{-1}
Preheating temperature	RT + 20–200 °C
Beam quality	M2 < 1.1
Optical structure	F–θ lens
Powder laying organization	One-way variable speed powder spreading
Minimum oxygen content	≤100 ppm
Protective gases	Ar/N_2

The mechanical properties of the three 316L stainless steel powder samples were evaluated by Vickers hardness values with a load of 1.0 kgf (HV1) and dwell time of 15 s. The average hardness value from over five data points was calculated per sample. The tensile samples were stretched at room temperature using a stretcher, and the stretching rate was set to 0.01 mm s^{-1}.

3 Results and discussion

3.1 Powder properties

Fig. 5 shows the surface spheroidization results after SLM forming with the three different powders. It could be seen that the mold surface of the aerosolized powder (Table 2, 3# powder) was relatively flat and there was no spheroidization; whereas the mold surface of the water-atomized powder (Table 2, 1# and 2# powder) has poor wettability and displayed strong spheroidization. It could also be seen that the influence of the powder properties on spheroidization was more obvious, and this could be analyzed from two aspects: one is the chemical properties of the powder, such as the oxygen content, and the chemical properties of the powder; and the other is the physical properties of the powder, such as its shape and packing density.

3.2 Oxygen content of the metal powders

The analysis in Fig. 6 shows that the total oxygen content of the powder influenced the balling effect more significantly. As the oxygen levels increased, the balling phenomenon increased. When using the 316L stainless steel powder (aerosolized) with a low oxygen content for laser melting, the mold surface was relatively flat, the single melting channel was more continuous, and the melting channel was well lapped, and there was still no large-area spheroidization phenomenon after the lapping (Fig. 6a). However, when using the 316L high-oxygen-content stainless steel powder (water atomization) for SLM testing, it was found that the single melting channel of the laser was discontinuous and divided into multiple metal balls, and the surface of the forming surface was relatively flat. The melting channel was also more continuous and divided into several metal balls. With multiple passes and multi-layer scanning, the formed surface eventually deteriorated and formed a large number of isolated large metal spheres (Fig. 6b–d). The quality of SLM forming could be seriously affected. Through the local magnification of Fig. 6b, as shown in Fig. 6c, it could be seen that a large amount of a white-like substance was distributed on the surface of the large metal balls (this substance was commonly found on the surface of SLM shaped samples). However, the amount and distribution of this white matter varied on the surface of samples molded with powders with different oxygen contents. Subsequently, EDX spectroscopy was performed to analyze this predominantly white matter, and an arbitrary area on the molded surface was analyzed, as shown in Fig. 7.

Fig. 8 shows the analysis of the micro-spheroidization on the surfaces of the SLM samples with different oxygen contents. It could be seen that the influence of the oxygen content of the metal powder on the spheroidization was not significant at the microscale. This was because, as analyzed in the previous

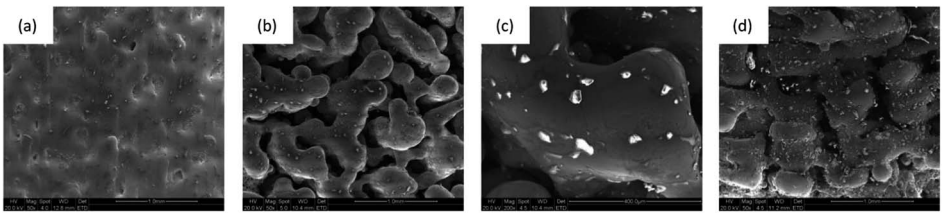

Fig. 6 Effect of 316L stainless steel powders with different oxygen contents (mole fraction) on large-size spheroidization of (a) aerosolized powder with 4.52% oxygen, (b) and (c) water-atomized powder with 5.44% oxygen; and (d) water atomized powder with 5.9% oxygen content.

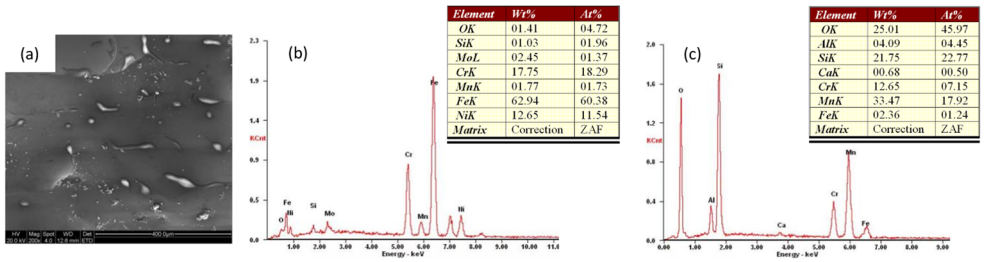

Fig. 7 Surface energy spectroscopy (EDX) analysis of SLM molding specimens: (a) surface SEM photo; (b) substrate EDX analysis; (c) white matter EDX analysis.

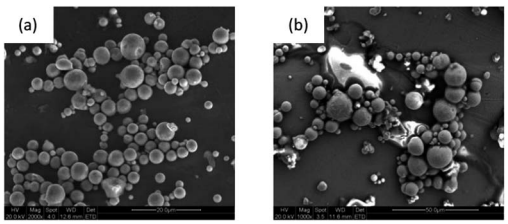

Fig. 8 Micro-size spheroidized SEM images of SLM formed specimen surfaces (a) 4.52% oxygen content and (b) 5.9% oxygen content.

section, microscale spheroidization occurred due to liquid metal splashing creating a large number of fine metal spheres under the action of the laser shock wave. In other words, the kinetic energy of the laser beam is partially converted into the surface energy of the sprayed metal balls, which in turn form a large number of fine metal balls, as shown in the figure. Thus, micro-spheroidization was related to the impact energy of the laser beam and not to the oxygen content of the metal powder. The large-area spheroidization was caused by the poor wettability due to the high oxygen content of the metal powder. Therefore, SLM molding materials should be selected from aerosolized powders with a low oxygen content to ensure the quality of SLM molding.

3.3 Mechanical property evaluation of samples with different oxygen contents

To investigate the mechanical properties of the 316L stainless steel fabricated by SLM, Vickers hardness and tensile strength tests were performed for the three samples, and the results are shown in Fig. 9. The mechanical properties of the three samples exhibited the highest value of 1350 ± 50 HV and tensile strength of 550 ± 20 MPa, which were comparable to the reported values fabricated by SLM.[32,33] The hardness value of the 1# sample first gradually decreased from 1100 ± 45 HV to 1010 ± 50 HV for the 2# sample and then increased to the highest value for 3# sample. The reason for the excessively high hardness of the 3# sample was its lowest oxygen content of 4.52%. Another likely reason was the fine average particle size of the 3# sample, because the smaller the particle size the better the effect of the laser melting. The ultimate tensile strength (UTS) was between 436 and 550 MPa, the yield strength (YS) was between 300 and 360 MPa, and the elongation (EL) was between 25% and 33%. The average UTS, YS, and EL values were 493 MPa, 330 MPa, and 28%, respectively. The mechanical properties were relatively good when the oxygen content was also the lowest at 4.52%. In addition to the low oxygen content and particle size, as shown in Fig. 6, another reason for the high hardness and strength is that the microstructure of the 3# sample was very uniform and fine.

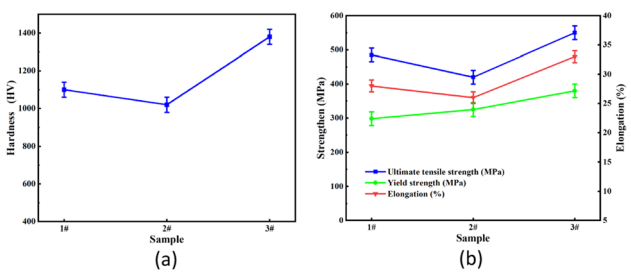

Fig. 9 Vickers hardness (a) and tensile properties (b) of the three samples.

4 Conclusions

This study investigated the spheroidization phenomenon produced by three types of 316L stainless steel powders with different manufacturing methods and different powder shapes when the shaped solids were subjected to SLM forming. The results show that the spheroidization phenomenon was not only related to the production method of the metal powder but also to the degree of wetting between the liquid metal and solid surface.

The main conclusions are as follows:

• In the process of forming a molten pool of metal powder, controlling the low oxygen content of 316L stainless steel powder can avoid the formation of oxides. At the same time, it can also form a clean wet surface, improve the wettability of the molten pool and substrate, and help avoid the occurrence of spheroidization. Therefore, the metal powder produced by atomization should be used in SLM forming because of its low oxygen atmosphere.

• By controlling the oxygen content of the metal powder and the SLM manufacturing method, we observed different surface morphologies. When the oxygen content was low, several small spherical particles appeared on the surface of the part when the metal powder was produced by atomization. When the oxygen

content was moderate and the metal powder was produced by water atomization, large and small spherical particles appeared on the surfaces of the parts. On the other hand, when a metal powder with a high oxygen content was prepared by water atomization, the surface of the parts showed a scattered distribution of large spherical particles and several small spherical particles. The above results show that a higher oxygen content can inhibit the formation of spheroidization.

• Under the action of laser energy and impact, the liquid metal was first melted and then splashed out due to the impact and the pressure difference between the molten pool, then forming small-sized balls after cooling. Spheroidization was related to the impact and pressure difference of the liquid metal in the forming process.

• The mechanical properties of the 3# sample displayed the highest value of 1350 ± 50 HV and tensile strength of 550 ± 20 MPa, which was the reason for the lowest oxygen content, fine average particle size, and very uniform and fine microstructure of the 3# sample.

Author contributions

Jibing Chen: conceptualization, methodology, validation, funding and acquisition. Yong She: writing – original draft, writing – review & editing. Xingyu Du: investigation, resources. Yanfeng Liu: data curation, visualization. Yang Yang: formal analysis, software. Junsheng Yang: supervision, project administration.

Conflicts of interest

There are no conflicts to declare.

Acknowledgements

Financial support from the Science and Technology Project of Science and Technology Department of Hubei Province (No. 2022EHB020) is gratefully acknowledged. The authors also acknowledge the Analytical and Testing Center of WHPU for their analytical work.

References

1 B. Nagarajan, Z. Hu, X. Song, W. Zhai and J. Wei, Development of micro selective laser melting: the state of the art and future perspectives, *Engineering*, 2019, **5**, 702–720.
2 A. K. Singla, M. Banerjee, A. Sharma, J. Singh, A. Bansal, M. K. Gupta, N. Khanna, A. S. Shahi and D. K. Goyal, Selective laser melting of Ti6Al4V alloy: process parameters, defects and post-treatments, *J. Adv. Manuf. Process.*, 2021, **64**, 161–187.
3 H. Meter and C. Haberland, Experimental studies on selective laser melting of metallic parts, *Mater. Sci. Technol.*, 2008, **39**, 665–670.
4 C. Galy, E. L. Guen, E. Lacoste and C. Arvieu, Main defects observed in aluminum alloy parts produced by SLM: from causes to consequences, *Addit. Manuf.*, 2018, **22**, 165–175.
5 X. Zhou, X. Liu, D. Zhang, Z. Shen and W. Liu, Balling phenomena in selective laser melted tungsten, *J. Mater. Process. Technol.*, 2015, **222**, 33–42.
6 M. Mazur, M. Leary, S. Sun, *et al*, Deformation and failure behaviour of Ti-6Al-4V lattice structures manufactured by selective laser melting (SLM), *Int. J. Adv. Des. Manuf. Technol.*, 2016, **84**, 1391–1411.
7 M. T. Andani, R. Dehghani, M. R. Karamooz-Ravari, R. Mirzaeifar and J. Ni, Spatter formation in selective laser melting process using multi-laser technology, *Mater. Des.*, 2017, **131**, 460–469.
8 D. Wang, S. Wu, F. Fu, S. Mai, Y. Yang, Y. Liu and C. Song, Mechanisms and characteristics of spatter generation in SLM processing and its effect on the properties, *Mater. Des.*, 2017, **117**, 121–130.
9 E. Liverani, S. Toschi, L. Ceschini and A. Fortunato, Effect of selective laser melting (SLM) process parameters on microstructure and mechanical properties of 316L austenitic stainless steel, *J. Mater. Process. Technol.*, 2017, 249.
10 S. Leuders, M. Thöne, A. Riemer, T. Niendorf, T. Tröster, H. A. Richard and H. J. Maier, On the mechanical behaviour of titanium alloy TiAl6V4 manufactured by selective laser melting: fatigue resistance and crack growth performance, *Int. J. Fatigue*, 2013, **48**, 300–307.
11 X. Zhou, X. Liu, D. Zhang, Z. Shen and W. Liu, Balling phenomena in selective laser melted tungsten, *J. Mater. Process. Technol.*, 2015, **222**, 33–42.
12 P. Oyar, Laser Sintering Technology and Balling Phenomenon, *Photomed. Laser Surg.*, 2018, 72–77.
13 R. Li, J. Liu, Y. Shi, *et al*, Balling behavior of stainless steel and nickel powder during selective laser melting process, *Int. J. Adv. Des. Manuf. Technol.*, 2012, **59**, 1025–1035.
14 S. Liu and H. Guo, Balling behavior of Selective Laser Melting (SLM) magnesium alloy, *Materials*, 2020, **13**, 3632.
15 J. Yang, J. Yu and Y. Huang, Recent developments in gelcasting of ceramics, *J. Eur. Ceram. Soc.*, 2011, **31**, 2569–2591.
16 M. Boutaous, X. Liu, D. A. Siginer and S. Xin, Balling phenomenon in metallic laser based 3D printing process, *Int. J. Therm. Sci.*, 2021, **167**, 107011.
17 D. Gu and Y. Shen, Balling phenomena in direct laser sintering of stainless steel powder: metallurgical mechanisms and control methods, *Mater. Des.*, 2009, **30**, 2903–2910.
18 Y. Qiu, J. Wu, A. Chen, P. Chen, Y. Yang, R. Liu, G. Chen, S. Chen, Y. Shi and C. Li, Balling phenomenon and cracks in alumina ceramics prepared by direct selective laser melting assisted with pressure treatment, *Ceram. Int.*, 2020, **46**, 13854–13861.
19 R. Li, Y. Shi, Z. Wang, L. Wang, J. Liu and W. Jiang, Densification behavior of gas and water atomized 316L stainless steel powder during selective laser melting, *Appl. Surf. Sci.*, 2010, **256**, 4350–4356.
20 X. Zhang, X. Dang and L. Yang, Study on balling phenomena in selective laser melting, *Laser Optoelectron. Prog.*, 2014, **51**, 061401.

21 J. P. Kruth, L. Froyen, J. V. Vaerenbergh, P. Mercelis, M. Rombouts and B. Lauwers, Selective laser melting of iron-based powder, *J. Mater. Process. Technol.*, 2004, **149**, 616–622.
22 J. P. Kruth, L. Froyen, J. V. Vaerenbergh, P. Mercelis, M. Rombouts and B. Lauwers, Selective laser melting of iron-based powder, *J. Mater. Process. Technol.*, 2004, 149.
23 E. Liverani, S. Toschi, L. Ceschini and A. Fortunato, Effect of selective laser melting (SLM) process parameters on microstructure and mechanical properties of 316L austenitic stainless steel, *J. Mater. Process. Technol.*, 2017, **249**, 255–263.
24 E. O. Olakanmi, R. F. Cochrane and K. W. Dalgarno, A review on selective laser sintering/melting (SLS/SLM) of aluminium alloy powders: processing, microstructure, and properties, *Prog. Mater. Sci.*, 2015, **74**, 401–477.
25 F. Trevisan, F. Calignano, M. Lorusso, J. Pakkanen, A. Aversa, E. P. Ambrosio, M. Lombardi, P. Fino and D. Manfredi, On the Selective Laser Melting (SLM) of the AlSi10Mg alloy: process, microstructure, and mechanical properties, *Materials*, 2017, **10**, 76.
26 H. Yu, S. Hayashi, K. Kakehi and Y. Kuo, Study of formed oxides in IN718 alloy during the fabrication by selective laser melting and electron beam melting, *Metals*, 2019, **9**, 19.
27 J. Krell, A. Röttger, K. Geenen and W. Theisen, General investigations on processing tool steel X40CrMoV5-1 with selective laser melting, *J. Mater. Process. Technol.*, 2018, **255**, 679–688.
28 B. Wysocki, P. Maj, A. Krawczyńska, K. Rożniatowski, J. Zdunek, K. J. Kurzydłowski and W. Święszkowski, Microstructure and mechanical properties investigation of CP titanium processed by selective laser melting (SLM), *J. Mater. Process. Technol.*, 2017, **241**, 13–23.
29 J. Chen, S. Yu, J. S. Yang, R. Xu, R. D. Li, S. Huang, H. Zhu and X. Liu, Research on the microstructure and mechanical properties of repaired 7N01 aluminum alloy by laser-directed energy deposition with Sc modified Al-Zn-Mg, *Metals*, 2023, **13**, 829.
30 J. Chen, N. Wan, J. Li and Z. He, Study on the polymer material infiltrating metallic parts by selective laser sintering of 3D printing, *Rapid Prototyp. J.*, 2018, **24**, 1539–1545.
31 J. Chen, J. Chen, J. Yang and Y. Wu, Selective laser sintering of acrylonitrile butadiene styrene polymer and post processing enhancement: an experimental study, *Iran. Polym. J.*, 2023, **32**, 1537–1550.
32 M. Higashi and T. Ozak, Selective laser melting of MoSiBTiC alloy with plasma-spheroidized powder: microstructure and mechanical property, *Mater. Charact.*, 2021, **172**, 110888.
33 G. Han, P. Wang, Y. Liu and W. Shi, Experiment of process strategy of selective laser melting forming metal nonhorizontal overhanging structure, *Metals*, 2019, **9**, 385.